Miniature Radar for Mobile Devices

Sharma, Praveen; Ouedraogo, Raoul; Perry, Bradley; Aubin, David; Levy, Todd; Souza, Daniel; Kitchens, Jonathan; Peabody, John
MIT Lincoln Laboratory, Lexington, MA 02420

Corresponding author: praveen.sharma@ll.mit.edu

Abstract

We developed a miniature and low-cost radar (radio detection and ranging) sensor for mobile devices. A radar differs from other mobile sensors - it provides diverse capabilities such as detection, tracking, ranging, and imaging. As a proof-of-concept for a radar sensor, we prototyped two X-band radars: using miniaturized X-band antennas: an X-band bi-static radar and time-division multiplexed, multiple-input multiple-output, and eight-elements phased-array radar. Using these radar sensors, we also demonstrated data acquisition and signal processing in real-time and supported both standalone and distributed applications. In particular, Range-Time-Intensity (RTI), Doppler-Time-Intensity (DTI), and Range-Angle-Intensity (RAI) were depicted as the illustrative signal processing algorithms, and Android smartphone was used as the illustrative processing platform.

Keywords: Smartphone, Miniature Radar, Signal Processing Algorithms, Standalone and Distributed Applications

I. Introduction

A. Motivation

Mobile devices have been emerging as excellent mobile-sensing platforms because they come with built-in sensors such as GPS antennas and accelerometers. Existing mobile-sensing applications either use these built-in sensors, or augment these built-in sensors with external sensors such as heart rate or perspiration monitors [1]. However, in most of these cases, mobile devices usually support applications in single domain, such as in health as shown in [1].

To enable mobile device support a wide-ranging applications such as in fire control and search and track, we report developing miniature and low-cost radar (radio detection and ranging) sensor for mobile devices; we used Android smartphone as the illustrative mobile device. Radars can support these multifarious applications because they provide diverse capabilities such as detection, tracking, velocity estimation, and imaging. Radar can also penetrate certain materials that are opaque to visible light, making it ideal for many applications like ranging through fog or even through walls [2].

B. Radar Background

Radars operate by transmitting electromagnetic radiation comprising a wide range of radio frequencies (RF) into an environment and receiving the subsequent reflections with precise timing. Since the radiation travels at the speed of light in free space, the round trip time determines the range of the scatters present in the environment. Utilizing multiple radar pulses can additionally yield information on target characteristics including speed and cross range.

The radar frequency bands of the RF spectrum are categorized in different bands, as shown in Figure 1. For this work S-band, C-band, and X-band radars were considered because of the size, cost, bandwidth and resolution tradeoffs that will be discussed shortly. We finally settled on X-band.

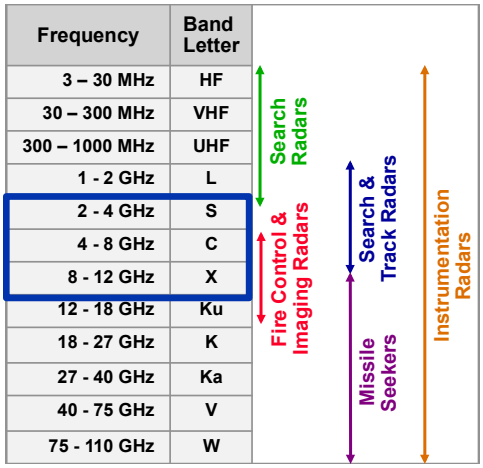

Figure 1: Division of the frequency spectrum for radars under IEEE STD 521-2002. RF spectrum in the blue rectangle is the focus of this paper

Various signal processing techniques can transform the radar measurements into other types of useful information like velocity estimates (Doppler processing), velocity filters, and depending upon the spatial aperture of the radar system, even angular estimates.

Radar systems come in all shapes, sizes, and price ranges. For example, high-resolution synthetic aperture imaging radars mounted on aircrafts are large and expensive whereas handheld radar guns that measure speed are relatively smaller and inexpensive A primary contributor to the price and size of the radar system is the operating frequency. The optimal size of the antenna elements of a radar system is inversely proportional to the operating frequency. The size constraint places a lower bound on the

This work is sponsored by the Department of the Air Force under Contract #FA8721-05-C-0002. Opinions, interpretations, conclusions and recommendations are those of the author and are not necessarily endorsed by the U.S. Government.

operating frequency for the smartphone radar. As the operating frequency becomes increasingly larger, the price of hardware increases; therefore, the price constraint places an upper bound on the operating frequency for reasonably priced radars for mobile devices.

C. Key Technical Contributions

This paper presents a design for a miniature, low-cost radar for mobile devices. As a proof-of-concept, we prototyped a miniature radar, and demonstrated radar functionalities by acquiring and processing signal in real-time. In particular, the prototype included:

1. Miniaturized antenna elements at X-band.
2. Prototypes of two X-band radars: bi-static radar and eight-elements, time-division multiplexed, multiple-input multiple-output (TDM-MIMO) phased array radar.
3. Range Time Intensity (RTI), Doppler Time Intensity (DTI), and Range Angle Intensity (RAI) signal processing algorithm implementations. RTI images the strength of the return signal at several range hypotheses over the radar's range extent sequentially over time; DTI images the strength of the return signal over several Doppler frequency (proportional to velocity) hypotheses sequentially over time; and RAI images the strength of the return signal over the range extent and several angular hypotheses.
4. A 3-D printed radar package.
5. Architecture supporting both standalone and distributed radar applications. For the former, the radar connects directly with a mobile device, and the device processes the algorithms using the CPU on the mobile devices. For the latter, the radar is paired with a GumStix, a peripheral embedded hardware with open Linux; it processes the algorithms, and makes the results accessible to a network of heterogeneous mobile or wired devices.

Note that X-band was chosen because this band provides a balance between size and cost. That is, it is relatively small in size, provides reasonably high bandwidth, and yet is relatively inexpensive.

D. Vision

As a long-term vision, one would miniaturize the radar under development and embed it within the mobile device. Since the Wi-Fi chip operates at 2.4 GHz, the chip should be able to toggle between serving as S-band radar and enabling wireless communications. However, in practice, designing this radar may require various hardware upgrades to mobile devices to support functionalities required by radar. Given time and budget constraints on the development, a lower risk proof-of-concept was undertaken.

The interim miniature radar interfaces to the mobile device and allows some of the functionality to be accomplished via external hardware. Even this interim radar should eventually be pluggable into mobile devices similar to how Universal Serial Bus (USB) interfaces with computing devices.

E. Paper Organization

The rest of the paper is organized as follows. Section II discusses related work. Section III sketches our process for prototyping. Section IV details antenna miniaturization and radar design and prototype. Section V summarizes the 3-D printing of the radar case. Section VI discusses prototyping of the signal-processing algorithms. Section VII describes standalone and distributed architectures. Section VII summarizes this work, and section IX presents future directions.

II. Related work

Because of the unique contributions of this effort, its comparison and contrast with other work is challenging. However, to provide a context, we attempt to relate this work with the following three diverse categories: integration of sensors with mobile devices, miniaturization of radar processing modules, and miniaturization of antennas.

A. Integration of Sensors with Mobile Devices

Several previous efforts integrate new or built-in sensors with mobile devices. Although sensors such as heart rate sensors [1], environmental pollution and radiation sensors [3], and temperature and humidity sensors [4] have been integrated with mobile devices, we do not know of any previous work that integrates radars with mobile devices. Unlike the existing sensors, radars can support diverse applications and vary in size. Furthermore, radar algorithms are CPU and memory intensive.

B. Miniaturization of the Radar Signal Processor

Relating radar miniaturization with similar efforts is also challenging because the operating frequency impacts the size of radars and the functionalities enabled by the radars. And, the existing miniature radars vary in frequency and size. As examples of these radars, consider the following. Delphi's Autonomous Cruise Control (ACC) radar [5] [6] is a miniature radar that operates at 76GHz and was used for long-range vehicle detection and lane crossing in DARPA's Urban Challenge [6]. Novelda impulse radar [7] is ultra-wideband radar that operates between 0.85GHz to 9.55 GHz and used for wide range of activities including collision detection. Another challenge with these commercial-of-the-shelf radars is that most of these, if not all, are proprietary thereby making it difficult to augment them with new signal processing algorithms.

C. Miniaturization of Antennas

Antennas are one of the most difficult components of a wireless system to miniaturize because conventional antennas operate properly when their dimensions are on the order of a half wavelength [8]. For the radar mobile-sensing applications, a compact, planar antenna with dimensions less than a quarter wavelength and at least 40% instantaneous bandwidth is desired. The dimensions of planar antennas can be reduced using techniques that involve the use of shorting plates or pins [9], slots [10], fractalization [11], and metamaterial loading [12]. Unfortunately, these miniaturizations techniques result in bandwidth reductions to values not suitable for our applications. To achieve both antenna miniaturization and bandwidth enhancement, a pixelization technique similar to that presented in [13] was employed in combination with the shorting plate approach of [9].

III. Prototype Design Decisions

This prototype was developed iteratively and design decisions such as selecting the frequency of the radar, ensuring the compatibility of the antenna elements with the chosen frequency bands, and determining the feasibility of executing signal processing algorithms on the mobile phone hardware versus peripheral hardware evolved throughout the project. A brief (chronological) reasoning underlying the design decisions follows.

Initially we focused on determining feasibility of executing the signal processing algorithms that lead to RTI and DTI displays on mobile phones. These algorithms rely on performing Fast Fourier Transforms (FFT). The FFT is known to be CPU and memory intensive, and underlies most of the signal processing algorithms. The initial implementation of these radars operating modes leveraged S-band coffee-can radar operating in the 2.40 – 2.48 GHz ISM band that was previously designed [14]. A success in this effort, albeit with several optimizations and lessons learned, enabled a move to test execution of RTI and DTI on a C-band coffee-can radar variant. This C-band radar was designed as an interim solution to test the feasibility of the algorithms before designing wider bandwidth X-band radar. Note that these changes were gradually moving towards a lower cost, smaller size, higher bandwidth and finer resolution radar.

After successfully executing RTI and DTI functions on the S-band and C-band radars, we investigated X-band radar and resource-intensive synthetic aperture radar (SAR) algorithm. For X-band operating at 10 GHz, the wavelength is 3 cm. For SAR at this wavelength, we would be required to position the phone at increments of no more than half the wavelength and collect data at each position. The more measurements we make, the wider our synthetic aperture becomes and the finer angular resolution we would achieve. We also make the assumption that the scene we are imaging is static over the timescale of the collection. It would be extremely difficult to align the mobile device radar using complimentary sensors like the built-in accelerometers because of the required precision in the position and orientation. This motivated a design of a Time Division Multiplexed – Multiple Input Multiple Output (TDM-MIMO) phased array radar. Collection of data from the phased array is referred to in this paper as a SAR collection because switching through the transmit-receive channel pairs individually forms the aperture. As a start for SAR prototyping, we began with Range Angle Intensity (RAI) images.

Finally, a decision to implement RAI on GumStix for the X-band radar was made because of the limitations of the FFT libraries for mobile devices and the challenges associated with the hardware available at the time for the standalone architecture.

IV. Antenna Miniaturization and Radar Architechture

A. Antenna Miniaturization

Typical antennas operating at X-band were either too large (exceeding ½") for this prototype or did not meet the bandwidth requirement of 40%. For instance, the X-band Horn antenna shown in Figure 2 meets the bandwidth requirements but it has dimensions of 1.27"x1.7"x2.82". To create planar compact antennas that meet both the size and bandwidth requirements, a pixelated bowtie antenna was designed.

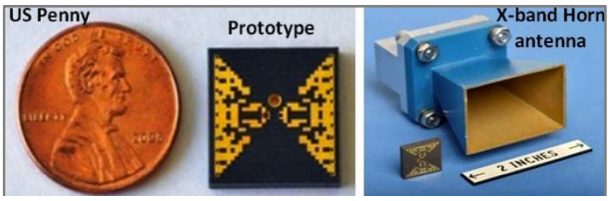

Figure 2: Prototype pixelated antenna next to US penny and X-band horn antenna for size reference

The design of this antenna began with a 0.5"x0.1"x0.5" bowtie antenna (Figure 3) that has an initial resonance at 17 GHz with a bandwidth of 18%. This antenna was then pixelated and the topology of the pixelization was optimized to shift the resonance down from 17 GHz. An iterative optimization algorithm was employed to maximize an objective function by toggling pixels on or off within the pixelated bowtie pattern. The resulting pattern that was manufactured is depicted in Figure 3. A photograph of the prototype antenna is shown in Figure 2. This antenna operates with more than 40% bandwidth, as was desired.

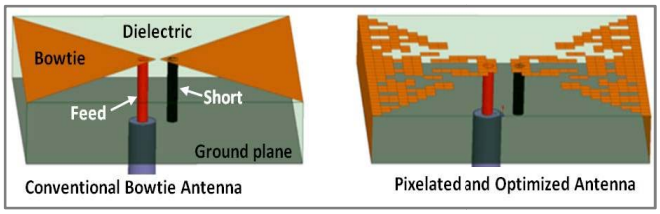

Figure 3: Conventional and pixelated bowtie antennas

Plots of the reflection coefficients of the pixelated and conventional bowties are shown in Figure 4. The operational bandwidth of an antenna is defined in this paper as the frequency band over which the reflection coefficient is less than -10dB, implying that less than 10% of the power is reflected from the antenna back to the generator.

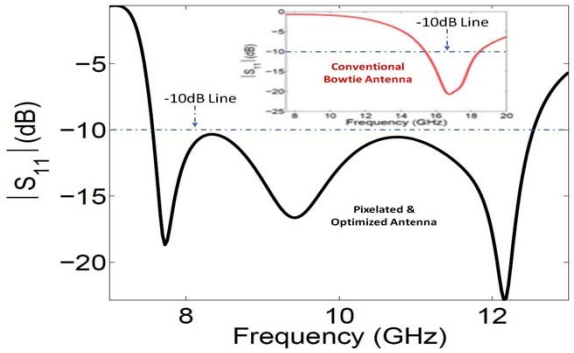

Figure 4: Reflection coefficient of optimized antenna (Inset figure shows reflection coefficients of initial antenna)

Plots of the realized gain of the pixelated antenna are shown in Figure 5. These antennas have a broad radiation characteristics, a gain of 5.5dBi, a front-to-back ratio of 8.5dB, and the cross polarization is below -30dBi.

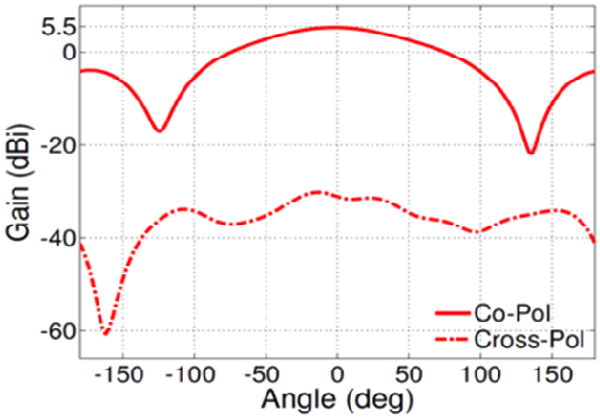

Figure 5: Radiation characteristics of the pixelated antenna

B. Radar Design and Prototype

Both the X-band radars utilize a pulsed linearly frequency modulated (LFM) transmit waveforms for ranging and continuous wave (CW) waveforms for Doppler.

Pulsed LFM was chosen because it allowed the use of the stretch processing architecture from the previously developed S-band coffee can [14] and phased array radars (Figure 6). Stretch processing was implemented to allow the utilization of high bandwidths to achieve fine range resolution while reducing the requirement on the sampling rate of the analog to digital converters (ADC).

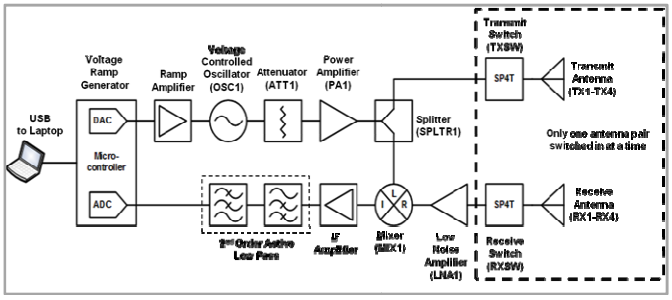

Figure 6: FMCW Radar Architecture

The X-band bi-static radar was designed and fabricated with a single transmit (Tx) and a single receive (Rx) antenna (Figure 7). The dimensions of the fabricated radar board is 2”x1”x0.2.”

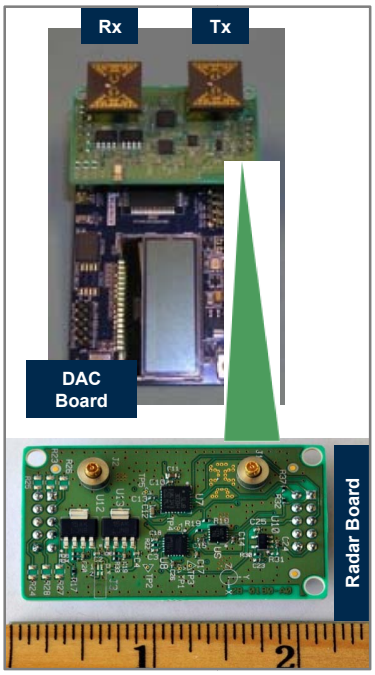

Figure 7: X-band bi-static radar

The X-band, eight-elements, TDM-MIMO phased-array radar was created with four Tx and four Rx, as shown in Figure 8. In this radar, the signal from the splitter goes through a single-pole quad-throw (SP4T) switch placed on the array board and only one of the four transmit antennas is excited at any given time. The four receive antennas are also connected to a single-pole quad-throw switch, and the

reflected signals received by the receive antennas are sent to the mixer one at a time.

The receive antennas are positioned at various intervals along a grid of one-wavelength spacing. The transmit antennas are positioned along a grid of two-wavelength spacing which is offset from the receive antenna spacing. Convolving these receive and transmit arrays yields a virtual array with fourteen unique bistatic-equivalent phase centers at one-wavelength spacing (Figure 8). Because the phase center spacing is larger than a half wavelength, grating lobes will be present when looking at high scan angles. The midpoints of the Tx/Rx pairs show the phase centers of the array prior to the convolution operation, which stretches it by a factor of two (Figure 9).

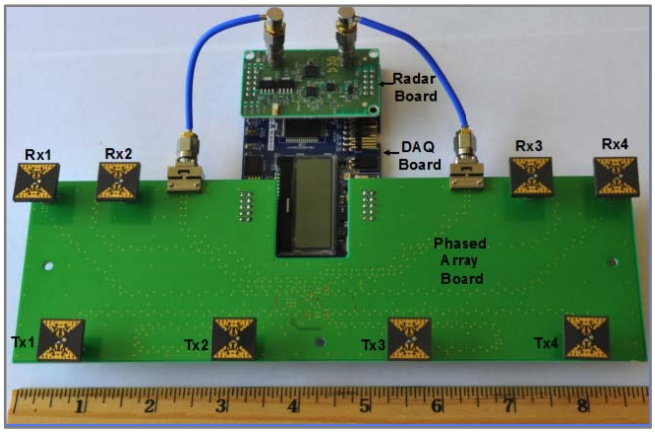

Figure 8: X-band, time-division multiplexed, multiple-input multiple-output phased-array radar

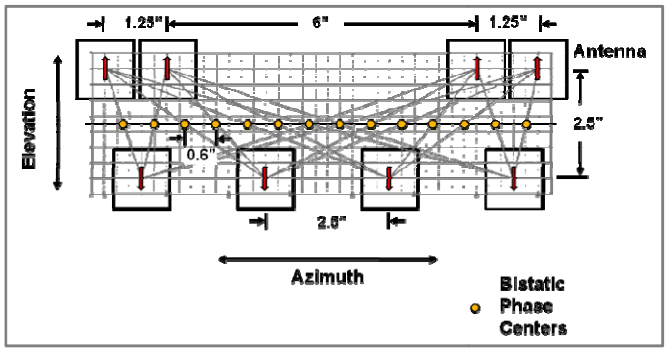

Figure 9: Bi- static radar antenna pair implementation

The fourteen Tx/Rx channels are swept from one end of the array to the other. For each channel pair, an LFM waveform with duration of 640 µs is transmitted and stretch processed. The total duration for all fourteen channels is 8.96 ms. The data for all of the channels is buffered and transmitted via USB all at once. This is done because the USB transfer has an associated nondeterministic delay. It is important to collect the data for each array channel quickly and uniformly to reduce the effects of angle-Doppler coupling and other artifacts. This process repeats throughout the duration that the array is in use. A diagram of the array timing is show in Figure 10.

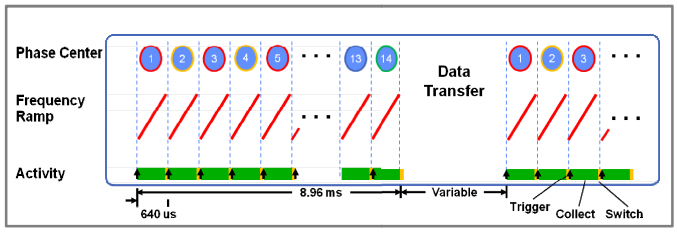

Figure 10: Array Timing

V. 3-D Printing Of Radar Platform

In addition to the board designs and prototyping, a 3-D printed package for both of the radars was designed and built. The case comprises modular containers for the antennas, the phased radar board, the microcontroller, batteries, the Wi-Fi antennas, the phones, the USB hub, and the GumStix (Figure 11). Figure 12 depicts the 3-D casing when all the components are assembled together.

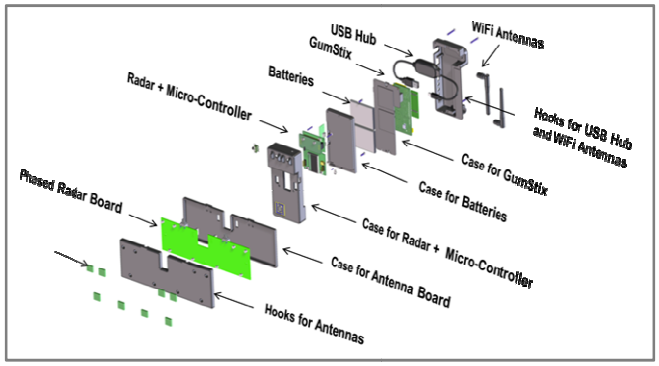

Figure 11: Modular 3-D printing of radar components

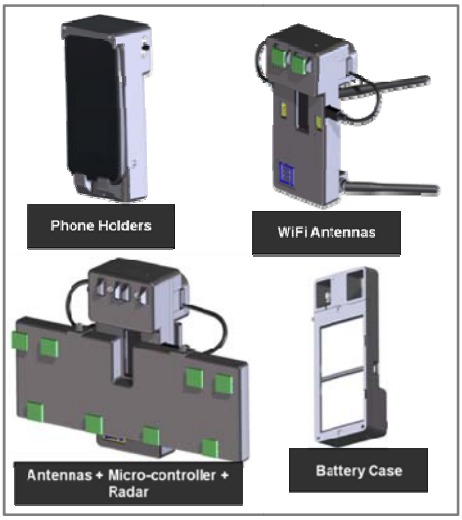

Figure 12: 3-D printed case with placeholders

VI. PROTOTYPE IMPLEMENTATION OF SIGNAL PROCESSING ALGORITHMS

As the illustrative signal processing algorithms, we prototyped the following three signal processing algorithms: Range Time Intensity (RTI), Doppler Time Intensity (DTI), and Range-Angle-Intensity (RAI), and developed displays for the algorithms.

A. Range-Time Intensity (RTI)

The RTI algorithm enables determination of the range of a target over a period of time. Utilizing stretch processing, the frequency of the processed return yields range information, shown in Figure 13 A, and is computed using equations 1 and 2. The return frequency is computed as the FFT ($\mathcal{F}$) of the time domain data vector x_i for each of the 14 channels.

$$\text{Intensity at each range hypothesis for channel i} = \mathcal{F}^{-1}\{x_i\} \quad (1)$$

$$\frac{\text{Frequency}}{\text{Chirp Rate}} = \text{Round Trip Delay} = \frac{2*\text{Range}}{\text{Speed of Light}} \quad (2)$$

B. Doppler-Time Intensity (DTI)

The DTI algorithm computes the Doppler frequency, which is proportional to the radial velocity as shown in Figure 13 B, and computed using equations 3 and 4 over time. This mode of operation uses a CW waveform as opposed to the pulsed LFM waveform that is used in the other modes. Objects with velocity components moving towards or away from the radar produce a Doppler frequency shift, which can be measured. Because this Doppler measurement approach utilizes a CW waveform, we are unable to simultaneously measure range in this mode. We are also only able to measure the magnitude of the velocity (speed) because the output frequencies are centered on 0 Hz after the mixing operation.

$$\text{Intensity} = \mathcal{F}^{-1}\{x\} \quad (3)$$

$$Doppler = \frac{2*Target\ Velocity}{wavelength} \quad (4)$$

C. Range-Angle-Intensity (RAI) Via Beam Formation

The RAI algorithm enables determining both range and the sine of the angle for each range-sin(angle) resolution cell. These polar coordinates can easily be mapped to Cartesian coordinates as well. The return frequency from the stretch processing maps to the range as in equation (1), and the sine of the angle is determined by the spatial frequency across the channels as shown in Figure 13 C and computed using equations 5 and 6, where dx is the distance between the phase centers. This algorithm includes two-pulse cancellation prior to the separable 2-Dimensional-FFT over the samples by channels matrix of data X.

$$\text{Intensity} = \mathcal{F}\{\mathcal{F}^{-1}\{X\}\} \quad (5)$$

$$\sin\theta = \frac{dx}{\text{wavelength}} \quad (6)$$

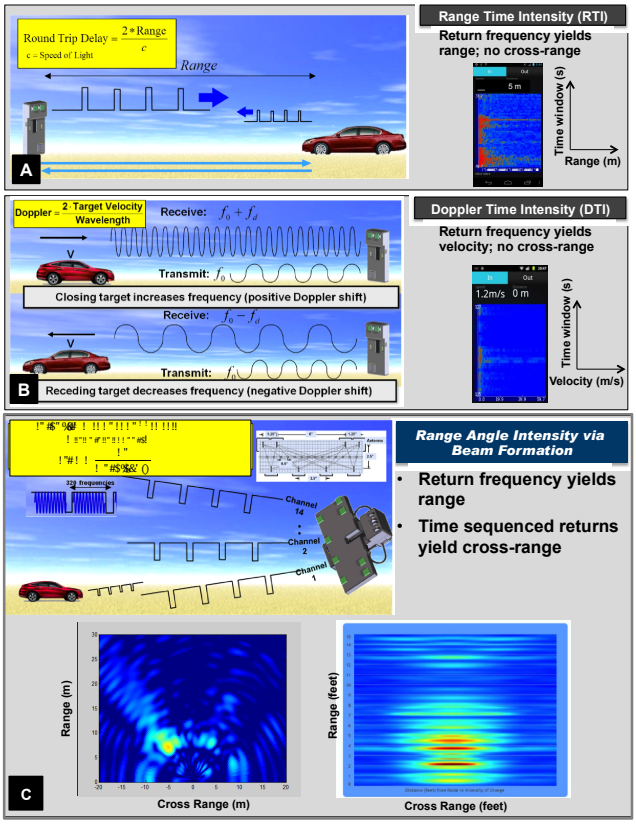

Figure 13: Signal processing algorithms: concepts and displays

D. Prototype Implementation

Android Samsung Galaxy Nexus is the smartphone that was used as the illustrative mobile device. GumStix was used as the illustrative embedded device running open Linux.

GumStix was selected for RAI for two primary reasons. First, GumStix supports Linux and porting signal processing libraries on to Linux is much easier than porting the libraries on the Android OS. Second, GumStix supports IEEE 802.11 protocol, which enabled untethered functionality as well as one-to-many cloud-like communications, one of the ways to support distributed applications.

For the signal processing libraries, the FFT and iFFT on the Android, SciMark [16] was utilized. For GumStix, custom libraries were constructed using Python's Math libraries. For evaluating both the SciMark and custom libraries, MATLAB libraries were used as a baseline.

E. Signal Processing Bottlenecks and Optimization

Several bottlenecks were encountered while running the signal processing algorithms on phones and processing had to be optimized to deal with these bottlenecks. The phones were both memory and CPU-bound.

These bottlenecks were addressed by limiting the input data to 600MHz of bandwidth, avoiding zero-padding the data prior to FFT, and considering the Goertzel Transformation [17] to limit the number of frequencies to be evaluated.

VII. Architectures

Architectures to enable the miniature low-cost radar we developed support both standalone and distributed operation were designed. A brief description of these architectures follows.

A. Standalone Architecture

In this architecture (Figure 14), the radar communicates with the smartphone via Seeeduino. Seeeduino translates analog to digital signal and uses the open Accessory Development Kit (ADK) protocol [18] to communicate with the smartphone. The smartphone executes the signal processing algorithms.

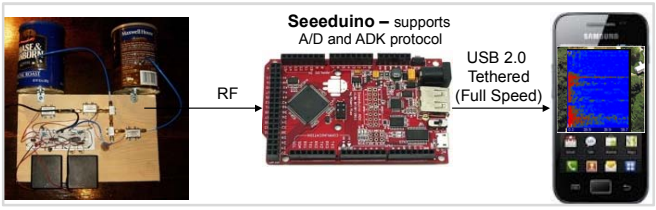

Figure 14: Standalone architecture

This architecture was used for processing RTI and DTI processing on the S-band radar with coffee can antennas and the C-band radar with spiral antennas.

Seeeduino was selected because it enabled 8-bit A/D conversion at the Nyquist rate for a 7.5KHz chirp generated every 40ms, and provided the best tradeoffs in size and functionality. Other options considered are listed in Table 1.

Several unanticipated issues were encountered using Seeeduino and the architecture was refined to address these issues. First, Seeeduino supported USB 2.0 only at full speed in a tethered mode. This constrained the data that could be transmitted between Seeeduino and the phone to be a theoretical maximum of 12 Mbps, and physically linked Seeeduino to the phone. Second, Seeeduino lacked support for threading and could not simultaneously perform Analog to Digital (A/D) conversion and transmit USB data. This made A/D processing and I/O potential bottlenecks. To compensate for the lack of threading, we considered an interrupt-driven architecture, and to reduce I/O wait time, two buffers of 2700Bytes were used. Finally, Seeeduino's inter-USB transmit time was 5 seconds introducing additional end-to-end latencies. This time was reduced to 10 microseconds and used our own proprietary protocol over ADK for communicating between Seeeduino and the phone.

Similar to Seeeduino, several issues were encountered with signal processing on Android phones. First, Android libraries did not have FFT functions that supported complex numbers. Second, although, the phone had a memory of 1GB RAM, each process is allocated only 56MB.

Table 1: Analog to Digital (A/D) alternatives

A/D Alternatives	Characteristics
Pure Arduino	Supports USB high speed for Android Samsung Nexus 4.0 only, which was not available at the time of this study
Yo-yo board	Provides low-sample rate of 1 KHz. To support Nyquist rate, we needed 15KHz
Raspberry Pi	No Wi-Fi, big form-factor, Unavailable at the time of this work
Phone's microphone	A/D quality was bad, and that it made the phone's microphone unusable

B. Distributed Architecture / Signal Processing in Cloud

For the distributed architecture (Figure 15), the radar communicates with GumStix via an X-Mega microcontroller. GumStix processes algorithms and the X-Mega card provides A/D conversion. Furthermore, any set of distributed devices can access the algorithms wirelessly using IEEE 802.11 protocol via a simple web-interface.

This architecture was used for the two-element, X-band radar and the eight-elements, X-band phased-array radar.

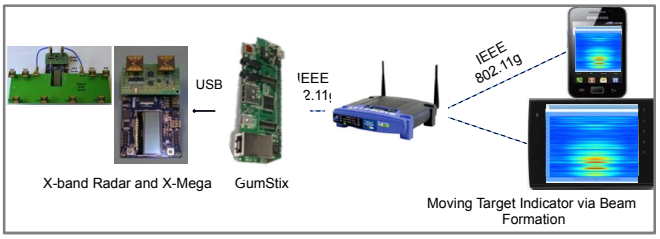

Figure 15: Distributed drchitecture

X-Mega was selected over Seeeduino because X-Mega provides both 12-bit A/D and Digital to Analog (D/A) conversion and Direct Memory Access (DMA) support. The A/D reliably utilized a clock rate of 500 kHz. GumStix was chosen over Android for processing algorithms because it supports Linux, which meant existing FFT libraries on Linux OS could be utilized. Table 2 compares resource characteristics of different hardware, including the phone, used in the paper.

Several additional issues were encountered with the processing hardware that should be noted. The X-Mega microprocessor was found to have a large amount of clock jitter, likely because USB heartbeats were used as the clock

instead of enabling the PLL module and using a different oscillator. GumStix did not simultaneously support USB and IEEE 802.11 protocol. And, although GumStix has a 700MHz ARM processor, it was severely CPU bound and could not produce more than 4 frames/second.

Table 2: Resource characteristics comparison

	Seeeduino	X-Mega	GumStix	Samsung Galaxy Nexus
CPU	16 MHz (8-bit) ATML AVR	24 MHz (16-bit) ATML AVR	700 MHz ARM Cortex-A8	1.2GHz ARM Cortex-A9, Dual Processor, 307 MHz Power/ GPU
Memory	8KB SRAM, no DMA	16KB SRAM, with DMA	512 MB RAM, 512 MB NAND	1 GB RAM, 512 MB SDRAM
A/D Sampling	10-bit 307 KHz	12-bit A/D & D/A with 1023 byte payload	N/A	N/A
USB 2.0 sampling rate	12Mbps, 8MHz	12 MHz	N/A	N/A

VIII. CONCLUSIONS

In this paper, we report developing a miniature low-cost radar as a versatile sensor for mobile devices. Radar is selected because it provides diverse capabilities ranging from detection, tracking, to image ranging and can support wide-ranging applications. As a proof-of-concept, we prototyped X-band bi-static radar using miniaturized X-band antennas, as well as an eight-elements, time-division multiplexed, multiple-input multiple-output phased-array radar. We also implemented and demonstrated data acquisition and signal processing in real-time for both standalone and distributed applications. In particular, range-time-intensity (RTI), Doppler-time-intensity (DTI), and range-angle-intensity (RAI) were depicted as the illustrative signal processing algorithms, and Android smartphone was used as the processing platform. Because, radar algorithms are CPU and memory intensive, various optimizations were implemented for the algorithms

IX. FUTURE DIRECTIONS

The radar board discussed here includes an Inertial Measurement Unit with sensors such as GPS and accelerometers. Although, these were not in this study, these sensors can be integrated to address requirements of several applications. Furthermore, A/D conversion, IEEE 802.11 and SDK protocols can be integrated in the radar board.

Furthermore, more work needs to be done in optimizing signal processing algorithms to operate on smartphones. As a start, sparse FFTs [19] needs to be evaluated for the radar reported in this paper.

X. REFERENCES

[1] D Lakens, "Using a Smartphone to measure heart rate changes during relived happiness and anger," IEEE Transactions of Affective Computing, PP, 99, 2013.

[2] G Charvat and J Peabody, "Real-time through-wall imaging using an ultra-wideband mulitple-input multiple-ouptput phased-array radar system," IEEE International Symposium on Phased Array Systems and Technology.551-558, 2010; http://www.ll.mit.edu/news/thruwallradar.html

[3] S Patterson, B Bamieh, and A E Abbadi, "Environmental tomography: uniquitous sensing with mobile devices," IEEE International Conference on Data Engineering, 2008.

[4] S. Aram, A Troiano, and E Pasero, "Environment sensing using smartphone, IEEE Sensors Applications Symposium," Feb 7-9, 2012.

[5] http://delphi.com/shared/pdf/ppd/safesec/acc.pdf

[6] http://people.csail.mit.edu/albert/pubs/2007-dgc-tech-report.pdf

[7] https://www.novelda.no/

[8] C. A. Balanis, *Modern Antenna Handbook.* Hoboken, NJ: Wiley, 2008

[9] K. L. Wong, *Compact and BroadbandMicrostrip Antennas*. Hoboken NJ: Wiley 2002

[10] S.A Bokhari, J F Zuercher, J R Mosig, and F E Gardiol, "A Small Microstrip Patch Antenna with a Convenient tuning option," IEEE Trans. Antennas Propag., vol. 44, no. 11, pp. 1521-1528, 1996.

[11] J P Gianvittorio and Y Rahmat-Samii, "Fractal Antennas: A Nonel Antenna Miniaturization Technique, and Applications," IEEE Trans. Antennas Propag. Mag., vol. 44, no. 1, pp. 20-36, 2002.

[12] R O Ouedraogo, E. J. Rothwell, A. R. Diaz, K. Fuchi, and A. Temme, "Miniaturization of Patch Antennas Using a Metamaterial-Inspired Technique," IEEE Trans. Antennas Propag. Mag., vol. 60, no. 5, pp. 2175-2182, 2012.

[13] R O Ouedraogo, E J Rothwell, A R Diaz, S Y Chen, . Fuchi, and A Temme, In Situ Optimization of metamaterial-inspired loop," IEEE Antennas Wireless Propag. Lett., vol. 9, pp. 75-78, 2010.

[14] G L Charvat, A J Fenn, B T Perry, "The MIT IAP Radar Course: build a small radar system capable of sensing range, doppler, and synthetic aperture (SAR) imaging." IEEE Radar Conference 2012, pp. 138-144.

[15] B T Perry, T Levy, P Bell, S Davis, K Kolodziej, J S Herd, "Low cost phased array for applications in engineering education". Accepted for publication – 2013 IEEE International Symposium on Phased Array Systems and Technologies

[16] SciMark 2.0 FFT Libraries; http://math.nist.gov/scimark2/

[17] G Goertzel, "An Algorithm for the Evaluation of Finite Trigonometric Series", *American Mathematical Monthly* **65** (1): 34–35, doi:10.2307/2310304, 1958

[18] ADK: http://developer.android.com/tools/adk/index.html

[19] H Hassanieh, P Indyk, D Katabi, and E Price, "Simple and Practical Algorithm for Sparse Fourier Transform." SODA, January 2012.